Study of eddy current power loss in an RCS vacuum chamber

XU Shou-Yan(许守彦) WANG Sheng(王生)[1)]

Institute of High Energy Physics (IHEP), Chinese Academy of Sciences, Beijing 100049, China

Abstract: In a Rapid Cycling Synchrotron (RCS), power loss due to an eddy current on the metal vacuum chamber would cause heating of the vacuum chamber. It is important to study the effect for estimating eddy current induced power loss and temperature growth. Analytical formulas for eddy current power loss for various types of vacuum chambers are derived for dipole and quadrupole repectively. By using the prototype of dipole of CSNS/RCS, an experiment was done to test the analytical formula. The derived formulas were applied to calculating the eddy current power loss on some special structures of an RCS vacuum chamber.

Key words: eddy current, power loss, vacuum chamber, RCS, CSNS

PACS: 41.20.q **DOI:** 10.1088/1674-1137/36/2/011

1 Introduction

In the Rapid Cycling Synchrotron (RCS), due to the rapid change of the magnetic field of dipoles and quadrupoles, a large eddy current is generated in the metal vacuum chamber, and the resulting power loss heats the duct. In the case of a large power loss, such as in the China Spallation Neutron Source (CSNS) RCS [1], with a high changing rate of magnetic field and large vacuum chamber aperture, heating becomes unacceptable. To decrease the heating effect, a ceramic chamber is usually adopted in the RCS main magnet, such as an RCS of the CSNS, ISIS [2] and J-PARC [3], and in the RCS with a smaller aperture or lower changing rate of magnetic field, such as in the KEK/PS [4] and Rapid Cycling Medical Synchrotron (RCMS) [5]. The heating effect can also be reduced to an acceptable level by adopting a bellows type vacuum chamber. It is important to study the effect and estimate the eddy current power loss on various types of vacuum chambers.

Analytical formulas for eddy current power loss on rectangular and elliptical uniform vacuum chambers in the dipole magnet have been derived by Y. Y. Lee and S. Y. Lee [6, 7]. In this paper, analytical formulas for eddy current power loss for various types of vacuum chambers, such as the bellows type vacuum chamber, are derived, not only for dipoles, but also for quadrupoles. By using the prototype dipole of CSNS/RCS, an experiment was done to test the analytical formula. The derived formulas were applied for calculating the eddy current power loss on some special structures of CSNS/RCS vacuum chamber, as well as the vacuum chamber of the Rapid Cycling Medical Synchrotron [8].

2 Analytical formulas for the eddy current power loss

2.1 Power loss on the vacuum chamber in the dipole magnet

2.1.1 Uniform vacuum chamber

The analytical formulas are derived starting from the elliptical uniform vacuum chamber in the dipole magnet. As shown in Fig. 1, the changing rate of the magnetic flux in two differential cells is $\dot{\Phi} = 2\dot{B}Lx$, and the voltage generated at the differential cell can be expressed by $\xi_0 = \dot{B}Lx$, the resistance $R_0 = L/\left[\sigma d\sqrt{1+y'^2}\cdot(\mathrm{d}x)\right]$, where σ is the electrical conductivity of the vacuum chamber material. One can get the power loss on each differential cell

$$p = \xi_0^2/R_0 = \dot{B}^2\sigma x^2 dL\sqrt{1+y'^2}\cdot(\mathrm{d}x). \qquad (1)$$

Received 18 May 2011

1) E-mail: wangs@ihep.ac.cn

The power loss on a quadrant of the elliptical vacuum chamber is

$$P_1 = \int_0^a \dot{B}^2 \sigma x^2 dL \sqrt{1+y'^2} \cdot \mathrm{d}x. \tag{2}$$

Because of the symmetry of the vacuum chamber, we get the eddy current power loss per unit length on the vacuum chamber

$$P = \frac{4P_1}{L} = 4\dot{B}^2 \sigma d a^3 \int_0^{\pi/2} \sin^2\theta \sqrt{1-\left(1-\frac{b^2}{a^2}\right)\sin^2\theta}\,\mathrm{d}\theta. \tag{3}$$

For $a > b$, Eq. (3) can be expressed as

$$P = \frac{4\dot{B}^2 \sigma d a^2 b}{3(a^2-b^2)} \left[(a^2-2b^2) E\left(1-\frac{a^2}{b^2}\right) + a^2 EK\left(1-\frac{a^2}{b^2}\right)\right], \tag{4}$$

where

$$E(k) = \int_0^{\frac{\pi}{2}} \sqrt{1-k\sin^2\theta}\,\mathrm{d}\theta$$

is the complete elliptical integral of the second kind,

$$EK(k) = \int_0^{\frac{\pi}{2}} \frac{1}{\sqrt{1-k\sin^2\theta}}\mathrm{d}\theta$$

is the complete elliptical integral of the first kind. When $a = b = r$, the vacuum chamber becomes the circular uniform vacuum chamber, and Eq. (3) is reduced to

$$P = \pi \dot{B}^2 \sigma d r^3. \tag{5}$$

For the rectangular uniform vacuum chamber, the formula can be derived in a similar way. The eddy current power loss per unit length on the rectangular uniform vacuum chamber in the dipole magnet is

$$P = \frac{2(P_1+P_2)}{L} = 4\dot{B}^2 \sigma a^2 d(b+a/3). \tag{6}$$

Eqs. (3) and (6) are the same as the formulas obtained by S. Y. Lee and Y. Y. Lee [6, 7].

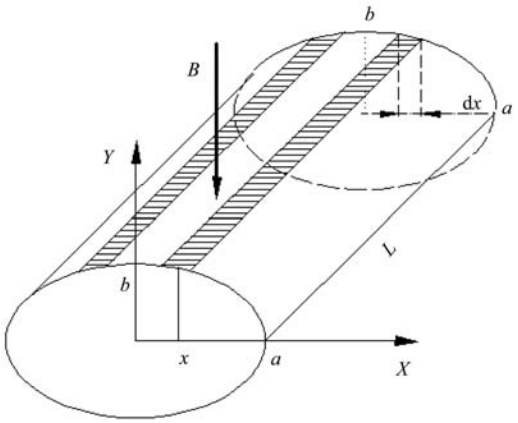

Fig. 1. The structure of the elliptical uniform vacuum chamber in the dipole magnet.

2.1.2 Bellows type vacuum chamber

Eddy current power loss can be reduced by using a bellows type vacuum chamber, such as used in the KEK/PS [4], and it also can be used in the RCS with a small aperture of vacuum chamber [5]. The eddy current power loss is studied in the dipole magnet for both edge welded bellows and hydroformed bellows.

First we consider the edge welded bellows. Let d be the thickness of the wall, $(h+2f)$ the height of corrugation, l the distance between two corrugations, and the cross section is an ellipse with a width of $2a$ and a height of $2b$, as shown in Fig. 2 and Fig. 3.

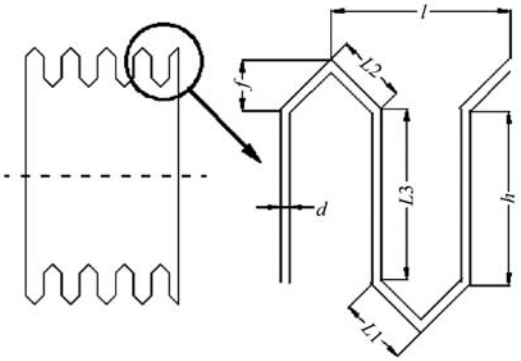

Fig. 2. The cross section along the longitudinal direction of the edge welded bellows type vacuum chamber.

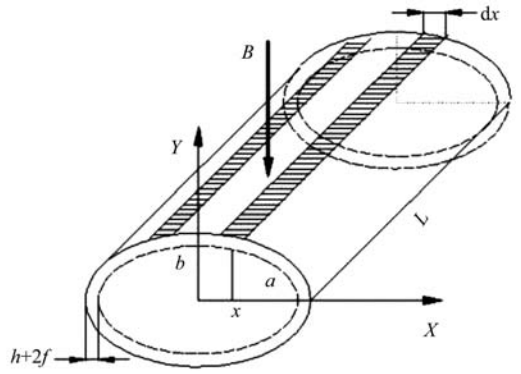

Fig. 3. The structure of the edge welded bellows type vacuum chamber in the dipole magnet.

The voltage generated at the differential cell in Fig. 3 can be given by

$$\xi_0 = \dot{B} L x \left(1+\frac{h}{2a}\right), \tag{7}$$

and the corresponding resistance is

$$R_0 = \frac{2L}{l}(R_1+R_2+R_3), \tag{8}$$

where R_1, R_2, R_3 correspond to the resistance of the sections with lengths of $L1$, $L2$, $L3$ respectively, as shown in Fig. 2. R_1, R_2, R_3 can be expressed as follows

$$\begin{aligned} R_1 &= \int_0^{l/4} \frac{4\sqrt{f^2+\frac{l^2}{16}}}{\sigma S l}\cdot \mathrm{d}z \\ &= \frac{4\sqrt{f^2+\frac{l^2}{16}}}{\sigma l d\sqrt{1+y'^2}\cdot \mathrm{d}x}\int_0^{l/4}\frac{\mathrm{d}z}{1+\frac{4fz}{la}} \\ &= \frac{a\sqrt{f^2+\frac{l^2}{16}}}{\sigma d f\sqrt{1+y'^2}\cdot \mathrm{d}x}\cdot \ln\left(1+\frac{f}{a}\right), \\ R_2 &= \frac{a\sqrt{f^2+\frac{l^2}{16}}}{\sigma d f\sqrt{1+y'^2}\cdot \mathrm{d}x}\cdot \ln\left(\frac{a+h+2f}{a+h+f}\right), \\ R_3 &= \frac{a+b}{2\sigma d\sqrt{1+y'^2}\cdot \mathrm{d}x}\cdot \ln\left(\frac{a+b+2f+2h}{a+b+2f}\right), \end{aligned}$$

where S is the area of transverse cross section of $L1$. In the case of $h, f \ll a,\ b$,

$$\xi_0 = \dot{B}Lx\left(1+\frac{h}{2a}\right) = \dot{B}Lx, \tag{9}$$

$$R_0 = \frac{2L}{l}(R_1+R_2+R_3) = \frac{2L\left(h+2\sqrt{f^2+\frac{l^2}{16}}\right)}{\sigma l d\sqrt{1+y'^2}\cdot \mathrm{d}x}. \tag{10}$$

One can get the power loss at each differential cell

$$p_0 = \xi_0^2/R_0 = \frac{\dot{B}^2x^2Lld\sigma\sqrt{1+y'^2}\cdot \mathrm{d}x}{2\left(h+2\sqrt{f^2+\frac{l^2}{16}}\right)}. \tag{11}$$

Then the power loss per unit length is

$$P = \frac{2\dot{B}^2 l d\sigma}{\left(h+2\sqrt{f^2+\frac{l^2}{16}}\right)}\int_0^a x^2\sqrt{1+y'^2}\mathrm{d}x. \tag{12}$$

For $a>b$, Eq. (12) can be expressed as

$$\begin{aligned} P &= \frac{2\dot{B}^2a^2bld\sigma}{3(a^2-b^2)\left(h+2\sqrt{f^2+\frac{l^2}{16}}\right)} \\ &\times\left[(a^2-2b^2)E\left(1-\frac{a^2}{b^2}\right)+a^2EK\left(1-\frac{a^2}{b^2}\right)\right]. \end{aligned} \tag{13}$$

For the circular chamber, $a=b=r$, and Eq. (12) is reduced to

$$P = \frac{\pi\dot{B}^2r^3ld\sigma}{2\left(h+2\sqrt{f^2+\frac{l^2}{16}}\right)}. \tag{14}$$

Comparing Eq. (13) and Eq. (14) with Eq. (4) and Eq. (5), an edge welded bellows type vacuum chamber can be equivalent to a uniform vacuum chamber with the thickness of

$$d_{\mathrm{e}} = \frac{ld}{2\left(h+2\sqrt{f^2+\frac{l^2}{16}}\right)}. \tag{15}$$

In the case of $l,\ f \ll h$, the equivalent thickness is reduced to

$$d_{\mathrm{e}} = \frac{l}{2h}d, \tag{16}$$

which is the same as the result in Ref. [4].

In a similar way, we can get the formula for hydroformed bellows. Let $l=4c$ be the distance between corrugations, and the corrugation height is $h+2c$. Fig. 4 shows the cross section along the longitudinal direction of the hydroformed bellows, while the cross section is the same as that shown in Fig. 3, where the corrugation height should be replaced by $h+2c$. Following a similar way of calculating the eddy current power loss at the differential cell, one can get the eddy current power loss per unit length on the elliptical hydroformed bellows ($a>b$) with $h,\ c \ll a,\ b$ in the dipole magnet

$$\begin{aligned} P &= \frac{8\dot{B}^2\sigma d a^2bc}{3(a^2-b^2)(\pi c+h)}\left[(a^2-2b^2)E\left(1-\frac{a^2}{b^2}\right)\right. \\ &\left.+a^2EK\left(1-\frac{a^2}{b^2}\right)\right]. \end{aligned} \tag{17}$$

For the circular hydroformed bellows, the eddy current power loss per unit length is

$$P = \frac{2\pi\dot{B}^2\sigma d r^3c}{\pi c+h}. \tag{18}$$

Comparing Eq. (17) and Eq. (18) with Eq. (4) and Eq. (5), a hydroformed bellows type vacuum chamber can be equivalent to a uniform vacuum chamber with a thickness of

$$d_{\mathrm{e}} = \frac{2cd}{h+\pi c}. \tag{19}$$

Compared with the uniform vacuum chamber, the resistance of the bellows type vacuum chamber is increased by using a bellows structure, and the eddy current power loss is reduced. By Eq. (13), Eq. (14), Eq. (17), and Eq. (18), the eddy current power loss on the bellows type vacuum chamber can be reduced by an increase in corrugation height and a decrease in the distance between two corrugations.

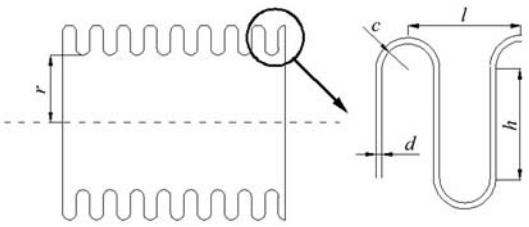

Fig. 4. The cross section along the longitudinal direction of the hydroformed bellows type vacuum chamber.

2.2 Power loss on the vacuum chamber in the quadrupole magnet

For the quadrupole magnet, we consider a circular vacuum chamber. For a circular uniform vacuum chamber, as shown in Fig. 5, let L be the length of the chamber, d the thickness, and r the radius of the cross section. The resistance of the differential cell shown in Fig. 5(b) is

$$R_0 = L/(\sigma dr \cdot \mathrm{d}\theta). \tag{20}$$

Let G be the gradient of the magnetic field, we can get the voltage generated at this cell

$$\xi_0 = \int_\theta^{\pi/4} \dot{G} r^2 L \sin 2\theta \cdot \mathrm{d}\theta = \frac{1}{2}\dot{G} r^2 L \cos 2\theta, \tag{21}$$

then the power loss on the differential cell is

$$p_0 = \frac{\xi_0^2}{R_0} = \frac{1}{4} L \dot{G}^2 r^5 \sigma d \cos^2 2\theta \cdot \mathrm{d}\theta. \tag{22}$$

The eddy current power loss at $\theta \in (0, \pi/4)$ is

$$P_1 = \int_0^{\pi/4} \frac{1}{4} L \dot{G}^2 r^5 \sigma d \cos^2 2\theta \cdot \mathrm{d}\theta = \frac{\pi}{32} L \dot{G}^2 r^5 \sigma d. \tag{23}$$

Due to the symmetry of the vacuum chamber, one can get the eddy current power loss per unit length

$$P = \frac{8P_1}{L} = \frac{\pi}{4} \dot{G}^2 r^5 \sigma d. \tag{24}$$

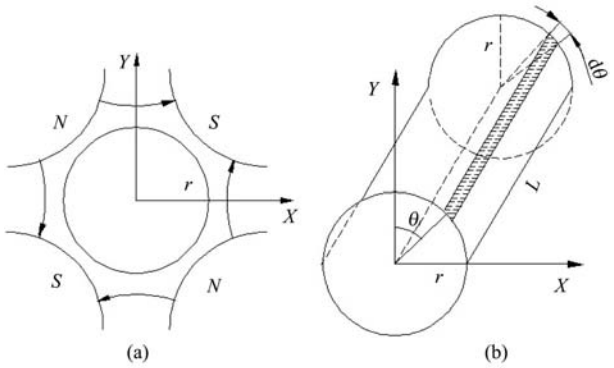

Fig. 5. (a) The cross section of the quadrupole magnet and the vacuum chamber; (b) The structure of the vacuum chamber.

Similarly, we can get the eddy current power loss per unit length on the circular edge welded bellows

$$P = \frac{\pi}{4} \dot{G}^2 r^5 \sigma d_\mathrm{e}, \tag{25}$$

where d_e is given by Eq. (15). In case of $h,\ c \ll r$, the formula for the circular hydroformed bellows in the quadrupole is given as

$$P = \frac{\pi \dot{G}^2 r^5 c \sigma d}{2(h + \pi c)} = \frac{\pi}{4} \dot{G}^2 r^5 \sigma d_\mathrm{e}, \tag{26}$$

where d_e is given by Eq. (19).

2.3 Eddy current power loss on a slice

The above-obtained analytical formulas can be applied to the long vacuum chamber only. For the very short chamber, such as the slice used for connecting two ceramic sections of vacuum chamber, the formulas do not work, and need to be re-derived. Fig. 6 shows a thin elliptical slice, with $L \ll a,\ b$, where L is the vacuum chamber length, and $a,\ b$ are the half width and height of the slice respectively.

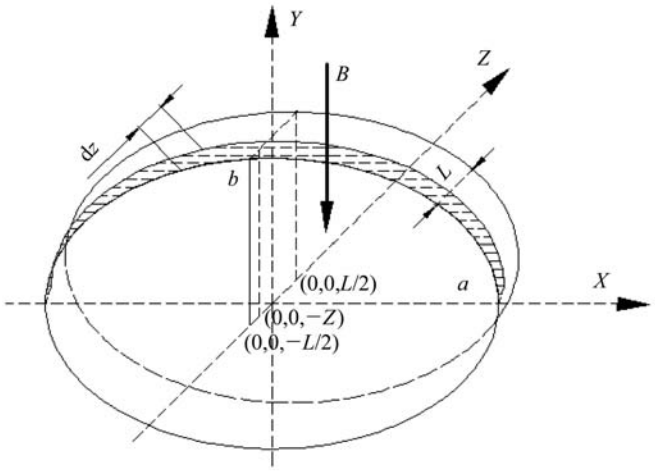

Fig. 6. A thin elliptical slice in the dipole magnet.

The voltage generated at the differential cell in Fig. 6 can be expressed as

$$\varepsilon = 2za\dot{B} \tag{27}$$

and the corresponding resistance can be expressed as

$$R = \frac{1}{\sigma d\cdot \mathrm{d}z}\int_{-\pi/2}^{\pi/2}\sqrt{a^2\cos^2\theta + b^2\sin^2\theta}\mathrm{d}\theta$$

$$= \frac{2a}{\sigma d\cdot \mathrm{d}z}E\left(1-\frac{b^2}{a^2}\right), \tag{28}$$

where d is the wall thickness of the vacuum chamber. Then we can get the power loss on the upper part of the vacuum chamber

$$P_1 = \frac{2a\dot{B}^2\sigma d}{E\left(1-\frac{b^2}{a^2}\right)}\int_{-L/2}^{L/2} z^2\,\mathrm{d}z = \frac{1}{6}\frac{a\dot{B}^2\sigma d L^3}{E\left(1-\frac{b^2}{a^2}\right)}, \tag{29}$$

and the power loss on the whole slice is

$$P = 2P_1 = \frac{1}{3}\frac{aL^3\dot{B}^2\sigma d}{E\left(1-\frac{b^2}{a^2}\right)}. \tag{30}$$

Figure 7 shows a thin circular slice in the quadrupole magnet, with $L \ll r$, where L is the vacuum chamber length, and r is the radius of the cross section of the slice. The voltage generated at the differential cell in Fig. 7 can be expressed as

$$\xi_0 = 2\int_0^{\pi/4}\dot{G}r^2 z\sin 2\theta\mathrm{d}\theta = \dot{G}r^2 z, \tag{31}$$

and the corresponding resistance can be expressed as:

$$R_0 = \frac{\pi r}{2\sigma d\cdot \mathrm{d}z}. \tag{32}$$

Then we get the eddy current power loss on the differential cell

$$p_0 = \frac{\xi_0^2}{R_0} = \frac{2\sigma\dot{G}^2 dr^3 z^2}{\pi}\cdot \mathrm{d}z. \tag{33}$$

The power loss on a quadrant of the thin circular slice is

$$P_1 = \int_{-L/2}^{L/2}\frac{2\sigma\dot{G}^2 dr^3 z^2}{\pi}\mathrm{d}z = \frac{\sigma\dot{G}^2 dr^3 L^3}{6\pi} \tag{34}$$

and the power loss on the whole slice is

$$P = 4P_1 = \frac{2\sigma\dot{G}^2 dr^3 L^3}{3\pi}. \tag{35}$$

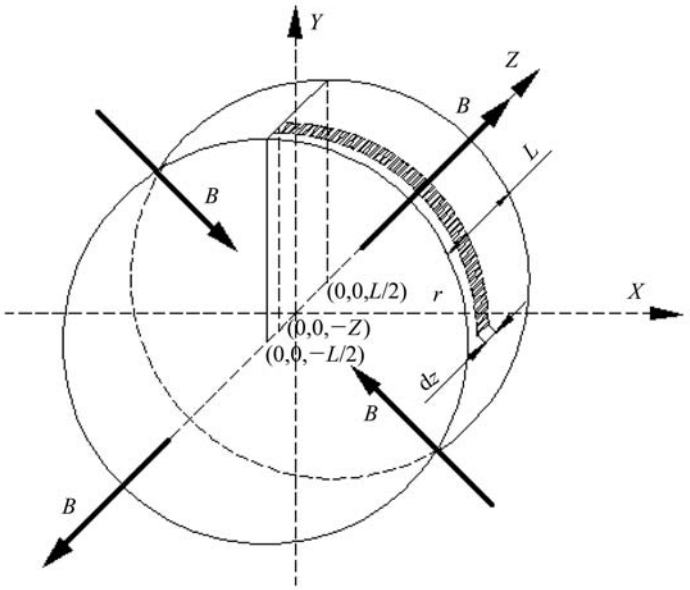

Fig. 7. A thin circular slice in the quadrupole magnet.

3 The experimental study of the eddy current power loss

The experiment was done for testing the eddy current power loss. The experiment was designed by using the prototype dipole of CSNS/RCS and a section of the metal duct. The dipole is powered by a resonant power supply with a repetition rate of 25 Hz. The vacuum duct is a section of stainless steel chamber used in the storage ring of the light source, made of 316L stainless steel with an elliptic cross section. The electrical conductivity of 316L stainless steel is $\sigma = 1.4\times10^6 S/m$. The thickness of the chamber is

d=0.7 mm, and the width and height are $2a$=55 mm, $2b$=31 mm respectively.

In the experiment, the dipole magnet operates at 25 Hz, in the form of $B(T) = D + A\sin 50\pi t$, powered by DC plus AC bias. Due to the eddy current effect, the temperature of the vacuum chamber rises until a heat transfer balance with the environment is achieved. The temperature sensors were used to measure the temperature of the vacuum chamber and the environment. The measured results are shown in Table 1, where T_0 is the environment temperature, and T_1 is the temperature of the vacuum chamber when heat transfer is balanced.

To theoretically calculate the temperature rise, first the eddy current power loss per unit length on the elliptical uniform vacuum chamber is calculated by using Eq. (4), then the temperature rise is simulated by using code ANSYS. With the given power loss on the vacuum chamber, the environment temperature, the thermal conductivity coefficient between the air and the vacuum chamber, and the convection heat transfer coefficient of the elliptical vacuum chamber, the final balance temperature of the vacuum chamber were obtained by simulation [9, 10].

Table 1 shows the calculated temperature rise, and the measured values, in which T_2 is the temperature obtained by simulation. The small difference between experiment and calculation may come from the error of the temperature sensor, which is about 1 ℃, and a not so accurate convection heat transfer coefficient used in the simulation. Considering these possible errors, the test results agree with the simulation results well.

Table 1. The simulation and test results. T_0 is the environment temperature, T_1 is the temperature of the vacuum chamber obtained by test, and T_2 is the temperature of the vacuum chamber by simulation.

magnet field/T	0.25+ 0.15sin50πt	0.30+ 0.20sin50πt	0.35+ 0.25sin50πt
power loss/ (W/m)	12.3	21.8	34
T_0/℃	29.5	29.5	31.0
T_1/℃	41.0	48.5	57.0
T_2/℃	39.0	44.9	53.4

4 Applications of formulas to CSNS and RCMS

4.1 Applications on CSNS

CSNS/RCS has a high changing rate of magnetic field and a large vacuum chamber aperture. The dipole magnet field is 0.16452 T at the injection and 0.98076 T at the extraction with a repetition rate of 25 Hz, and the largest variation of gradient of quadrupole is from 1.1 T/m to 6.6 T/m. The vacuum chambers in the dipole magnets have an elliptical cross-section of 216 mm×134 mm, and those in the quadrupole magnets have a circular cross-section of radius 118 mm.

Table 2. The eddy current power losses on the duct joints (with an electrical conductivity of 1.7×10^8 S/m).

magnet	power loss/W
dipole	0.1
quadrupole	0.03

Table 3. The eddy current power losses per unit length on the TiN film (with an electrical conductivity of 5.88×10^6 S/m).

magnet type	thickness of the TiN film/nm	power loss/(W/m)
quadrupole	20	0.2
quadrupole	60	0.6
quadrupole	100	1.0
dipole	20	0.7
dipole	60	2.1
dipole	100	3.5

Since the eddy current power loss on a metal vacuum chamber produces an unacceptable power loss, the vacuum chambers made of ceramic are adopted in the dipole and quadrupole magnets. The segments of ceramic are jointed by brazing with a copper slice to form a long vacuum chamber, and the segment wall thickness is 10 mm. The thickness of the slice is L=1 mm, as shown in Fig. 6 and Fig. 7. The eddy current power loss on the copper slice between two ceramic segments is calculated by using Eq. (30) and Eq. (35). The calculated results are shown in Table 2.

In order to reduce emission of secondary electrons when protons or electrons strike the surface, TiN film is coated on the inner surface of the ducts. By using Eq. (4) and (24), the eddy current power losses per unit length on the TiN film in the dipole magnet and quadrupole magnet are calculated, as shown in Table 3.

4.2 Applications in RCMS

Another application of these formulas is for the vacuum chamber used in the Rapid Cycling Medical

Synchrotron (RCMS). In [10], the hydroformed bellows type vacuum chamber, made of inconel625, is adopted. The cross section of the vacuum chamber is an ellipse with a width $2a$=50 mm and height $2b$=35 mm. By using Eq. (15), the eddy current power loss for the bellows in a dipole magnet is calculated, as shown in Table 4. As the size of the vacuum chamber is much smaller than that of CSNS/RCS, it is possible to use the bellows type vacuum chamber in this kind of RCS. The parameters of hydraulic bellows used in the calculation are c=0.625 mm, h=1.25 mm, (c, h are shown in Fig. 4).

Table 4. The eddy current power losses per unit length on the bellows type vacuum chamber in the dipole magnet (The electrical conductivity of inconel625 is $\sigma = 0.8 \times 10^6$ S/m).

thickness of the vacuum chamber/mm	magnet field/T	power loss/ (W/m)
0.15	0.73+0.53sin50πt	6.03

5 Summary

The analytical formulas for the eddy current power loss on various types of vacuum chambers are derived. Experiments are done to test the analytical formulas. By using the analytical formulas, the eddy current power losses of vacuum components for CSNS/RCS and a bellows type vacuum chamber used in the RCMS are estimated.

References

1 WANG S et al. Chinese Physics C (HEP & NP), 2009, **33**(S2): 1–3
2 Bennett J, Elsey R, Dossett A. Vacuum, 1978, **28**: 507–509
3 Kinsho M et al. Vacuum, 2004, **73**: 187–193
4 Horikoshi G et al. Vacuum System for the KEK Proton Synchrotron, PAC1977
5 Gardner C et al. Conceptual Design of the RCMS, BNL. 2003
6 Lee Y Y. Estimate of Eddy Current Power Loss in the Dipole Vacuum Chamber, Booster Technical Note 51, Brookhaven National Laboratory. 1986
7 Lee S Y. Nuclear Instruments and Methods in Physics Research A, 1991, **300**: 151–158
8 Conceptual Design Report of Energy Modulation Ion Therapy Facility. IHEP-Report, May, 2008
9 HUANG S Y, PU S Z. Heat and Mass Transfer, 1995, **30**: 411–415
10 YANG S M, TAO W S. Heat Transfer Theory, Higher Education Press of China. 1998